# Chemical Vapor Deposition of Lithium Phosphate Thin-Films for 3D All-Solid-State Li-Ion Batteries

**Jie Xie,[a] Jos F. M. Oudenhoven,[b,*] Peter-Paul R. M. L. Harks,[a] Dongjiang Li,[a,c] and Peter H. L. Notten[a,d,*,z]**

[a]*Eindhoven University of Technology, 5600 MB Eindhoven, The Netherlands*
[b]*Holst Centre - imec, 5656 AE Eindhoven, The Netherlands*
[c]*School of Energy Research, Xiamen University, Xiamen 361005, People's Republic of China*
[d]*Forschungszentrum Jülich IEK-9, D-52425 Jülich, Germany*

High quality Lithium phosphate ($Li_3PO_4$) thin films have been deposited by metal-organic chemical vapor deposition (MOCVD), using tert-butyllithium and trimethyl phosphate as precursors. The $Li_3PO_4$ films deposited at 300°C yielded the highest ionic conductivity ($3.9 \times 10^{-8}$ S · cm$^{-1}$). Increasing the deposition temperature led to crystallization of the deposited films and, consequently, to lower ionic conductivities. Kinetic studies on planar substrates showed that $Li_3PO_4$ deposition is a diffusion-controlled process in the temperature range of 300 to 500°C. $Li_3PO_4$ films have also been deposited on highly structured substrates to investigate, for the first time, the feasibility of 3D deposition of $Li_3PO_4$ by MOCVD. Furthermore, very thin films of $Li_3PO_4$ have been deposited onto thin film Si anodes and it was found that these layers effectively suppress the SEI formation and dramatically improve the cycle performance of Si film anodes.


Manuscript submitted October 22, 2014; revised manuscript received November 25, 2014. Published December 9, 2014.

Driven by the fast development of autonomous devices, all-solid-state micro-batteries currently attract a lot of attention. The three dimensional (3D) all-solid-state Li-ion battery is a challenging concept, which will significantly improve the volumetric capacity and rate capability of micro-batteries.[1–3] A stable thin film electrolyte is one of the important components for micro-batteries. Due to the relatively high Li-ion conductivity and (electro)chemical stability upon contact with Li anodes,[4] lithium phosphate thin films are among the most popularly used electrolytes for micro-batteries.

Lithium phosphate based thin film electrolytes are generally deposited by sputtering,[4–7] pulsed laser deposition[8] and E-beam evaporation.[9] Because of shadow effects, these methods are hardly suitable for 3D deposition. In addition, during the deposition process using these methods, there is a temperature difference between the substrate and the deposited films. The resulting thermal tensile stress may disadvantageously cause film cracking.[10]

Atomic layer deposition (ALD) and metal-organic chemical vapor deposition (MOCVD) are two methods that can deposit very homogeneous and conformal films on highly structured substrates. Unfortunately, the ALD method is relatively slow[11] and therefore rather unpractical for the deposition of battery materials. Several papers reported the chemical vapor deposition of nitrogen doped lithium phosphate[10,12] but none of these papers explored the feasibility of deposition in 3D. In this study, MOCVD is investigated to deposit $Li_3PO_4$ thin films, using tert-butyllithium (t-BuLi) and trimethyl phosphate (TMPO) as precursors. The MOCVD process for $Li_3PO_4$ thin film deposition has been developed and the influence of the substrate temperature on the morphology, crystal structure and ionic conductivity has been systematically studied. In order to investigate the feasibility of three dimensional deposition of $Li_3PO_4$ by MOCVD, thin films were also deposited onto highly-structured substrates. The thickness development of the deposited thin films inside these 3D-structures has been investigated.

In addition, the deposited $Li_3PO_4$ films were applied as protective layer on top of Si thin film anodes. It will be shown that very thin $Li_3PO_4$ layers can effectively suppress the SEI formation and, consequently, dramatically improve the cycle life performance.

## Experimental

*Thin film deposition.*— The MOCVD setup used for $Li_3PO_4$ deposition has been described in detail in a previous publication.[13] In short, a cold wall low pressure MOCVD reactor (Aixtron 200 RF) was used, in which the sample substrate was positioned on a radio frequency heated susceptor. The precurors were trimethyl phosphate (TMPO) and tert-butyllithium (t-BuLi), both acquired from SAFC-Hitech (United Kingdom). Preliminary parametric variation experiments were first carried out to find the base operating conditions, including the bubbler temperatures and carrier gas flow rates, which are listed in Table I. Argon was used as carrying gas.

$Li_3PO_4$ layers for thickness and surface morphology analyses were deposited onto square silicon substrates with a width of 3 cm. The $Li_3PO_4$ samples prepared for the electrochemical measurements were deposited on similar substrates covered with a barrier layer of TiN and a layer of platinum (Si/TiN/Pt). For the impedance measurements to be conducted after $Li_3PO_4$ deposition, nine Pt dots with a diameter of 3 mm and thickness of 200 nm were deposited on top of the $Li_3PO_4$ films by masked sputter deposition.

To investigate the feasibility of 3D deposition, $Li_3PO_4$ films were deposited onto silicon wafers which were reactive ion etched to obtain trenches with a width and depth of 30 μm. $Li_3PO_4$ thin films were also deposited as protective layers onto 50 nm thick Si layers. The Si anodes were deposited on TiN-covered (70 nm) Si-substrates by electron beam evaporation. A mask was used during the E-beam process to confine the Si film area to 2 cm$^2$. Subsequently, the whole substrate was covered with 200 nm $Li_3PO_4$.

*Sample characterization.*— Thickness and morphology of the $Li_3PO_4$ thin films were measured using a scanning electron microscope (SEM, Philips/FEI XL 40 FEG). The structural properties of the $Li_3PO_4$ films were investigated by an X-ray diffractometer (XRD, Panalytical X'Pert PRO MPD).

The electrochemical and impedance measurements were performed in an argon-filled glove box ($O_2$ and $H_2O$ < 1 ppm). An Autolab PGSTAT 302 (Metrohm-Autolab B.V., The Netherlands) and a two electrodes setup were used to carry out the impedance measurements on the Pt/$Li_3PO_4$/Pt stacks. For potentiostatic cyclic voltammetry (CV) and galvanostatic cycling (GC) measurements, the samples were positioned in Teflon cells and used as working electrodes. Lithium metal foils were utilized as reference and counter electrodes. The cell was filled with 1 M $LiClO_4$ in propylene carbonate (Soulbrain MI, United States). This three-electrodes setup was connected

*Electrochemical Society Active Member.
[z]E-mail: p.h.l.notten@tue.nl

**Table I. MOCVD process parameters for $Li_3PO_4$ deposition.**

| Precursor | Temperature °C | Pressure *mbar* | Flow *cc/min* |
|---|---|---|---|
| t-BuLi | 50 | 400 | 400 |
| TMPO | 20 | 500 | 40 |
| Oxygen | Room temperature | | 1 |
| Total gas flow | Room temperature | | 1550 |

to an Autolab to perform cyclic voltammetry or a M2300 galvanostat (Maccor, Tulsa, USA) to perform galvanostatic (dis)charging. Cyclic voltammetry was executed at 1 mV/s and all potentials are given vs the $Li/Li^+$ reference electrode. The constant current experiments were performed at a rate of 1 C (80 μA). All electrochemical tests were carried out at room temperature.

## Results and Discussion

Fig. 1a shows the deposited film thickness as a function of deposition time. The film thickness increases linearly with deposition time, indicating that the deposition rate is constant during the deposition process at 350 and 500°C, which makes controlling the film thickness straightforward. The slopes of the two lines are almost equal. This suggests that the deposition temperature does not have a clear influence on the growth rate of $Li_3PO_4$ thin films, which is further confirmed by the Arrhenius plot, shown in Fig. 1b. In the entire temperature range (300 ∼ 500°C), the deposition rate is only weakly dependent on the deposition temperature. The activation energy calculated from Fig. 1b is 1.14 kJ/mole, which is very low. Consequently, the MOCVD deposition of $Li_3PO_4$ is considered to be diffusion-controlled in the studied deposition temperature range.

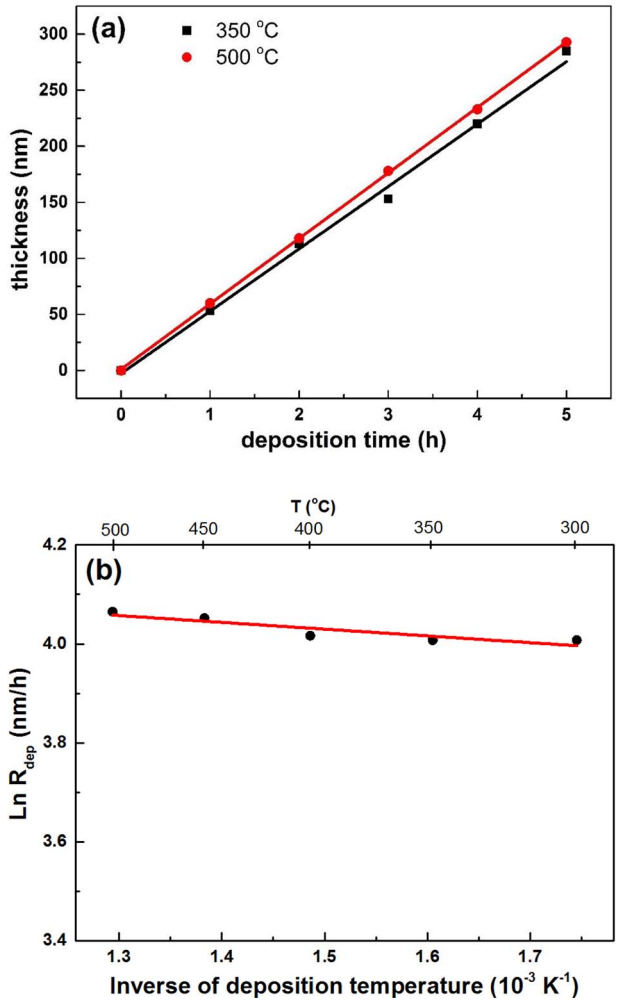


**Figure 1.** Deposited film thickness as a function of deposition time at 350°C and 500°C (a) and Arrhenius plot for the deposition rate of $Li_3PO_4$ films (b).

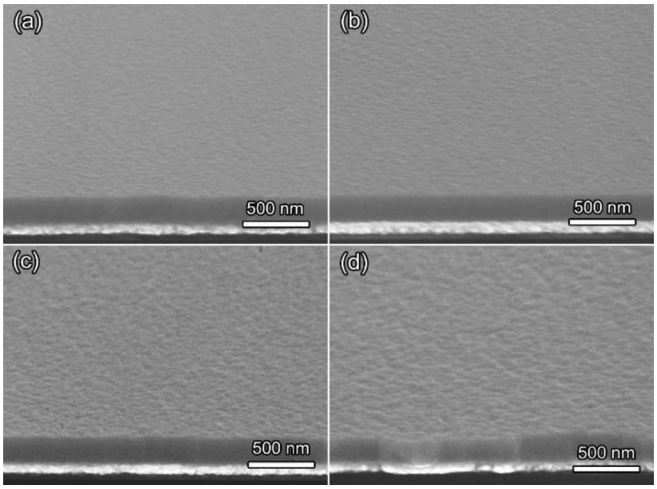


**Figure 2.** SEM images of $Li_3PO_4$ thin films deposited at different temperatures 300°C (a), 350°C (b), 400°C (c) and 450°C (d).

Fig. 2 shows the morphology of the thin films deposited at different temperatures. The MOCVD deposited $Li_3PO_4$ films are very homogeneous, without revealing any cracks or pinholes. Looking into more detail, it can be concluded that the surface becomes somewhat rougher with increasing deposition temperature. It appears that the $Li_3PO_4$ films deposited at higher temperatures are polycrystalline, forming grain boundaries. To confirm this, grazing incidence XRD was conducted.

Fig. 3 shows the XRD patterns of $Li_3PO_4$ films deposited at different temperatures. The XRD pattern of the films deposited at 300°C (black curve) shows no clear reflections, except for the Pt peaks originating from the substrate. The XRD diffraction pattern of the films deposited at 350°C (red curve) shows a bump at around $2\theta = 24°$, where two strong reflections of $Li_3PO_4$ (PDF 25–1030), (101) and (011), are located. This indicates that at 350°C, the deposited $Li_3PO_4$ film is partially crystalized, but the crystal structure is not well developed. Another reason might be that the formed $Li_3PO_4$ particles are very small, which give rise to broad reflections. For the films

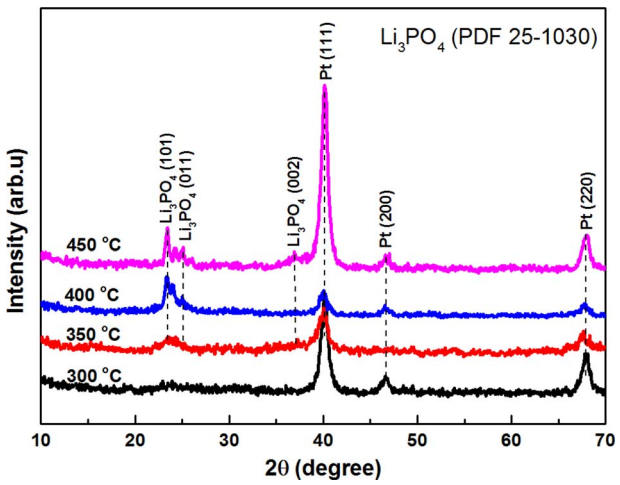


**Figure 3.** XRD patterns of $Li_3PO_4$ films deposited at 300, 350, 400 and 450°C.

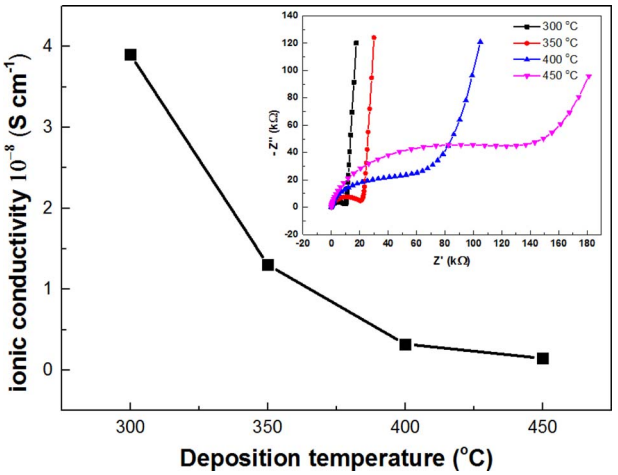


**Figure 4.** Ionic conductivity of $Li_3PO_4$ films as a function of deposition temperatures. The inset shows the corresponding impedance plots.

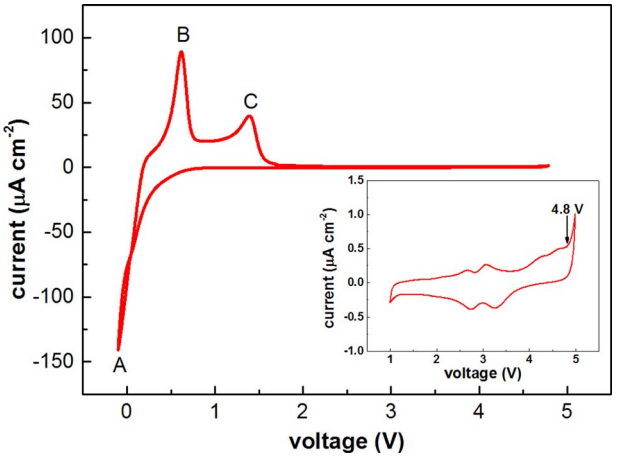


**Figure 5.** Cyclic voltammogram of a Pt/ $Li_3PO_4$ /Li half-cell at room temperature. The insert shows the scan range between 1 ∼ 5 V.

deposited at higher temperatures, characteristic peaks of $Li_3PO_4$ can be observed. Further increase of the deposition temperature to 450°C (magenta curve) makes the $Li_3PO_4$ films more crystalline. Another peak assigned to $Li_3PO_4$ (002) appears in this diffractogram at $2\theta = 37^\circ$. The XRD results confirm that the $Li_3PO_4$ deposited at lower temperatures is amorphous and becomes (partially) crystalline at higher deposition temperatures, which is consistent with the morphology development observed in the SEM images shown in Fig. 2.

Ionic conductivity is one of the most important properties of solid-state electrolytes. Electrochemical impedance spectroscopy (see the inset of Fig. 4) was used to determine the ionic conductivity of the deposited $Li_3PO_4$ thin films. The ionic conductivity ($\sigma$) is calculated according to

$$\sigma = \frac{d}{A \times R}, \qquad [1]$$

where $d$ is the thickness of the lithium phosphate film, $A$ is the area of the electrode, and $R$ is the resistance which is evaluated by measuring the diameter of a semi-circle in the measured impedance spectra. As shown in Fig. 4, the film deposited at 300°C has the highest ionic conductivity of $3.9 \times 10^{-8}$ S · cm$^{-1}$, which is well within the range of reported values.[4,6] When the deposition temperature is set at 350°C, the ionic conductivity dramatically drops. At a deposition temperature of 400°C, the ionic conductivity stabilizes at around $3 \times 10^{-9}$ S · cm$^{-1}$. Further increasing the deposition temperature to 450°C only slightly affects the ionic conductivity. It is well known that amorphous $Li_3PO_4$ has a better ionic conductivity than the crystallized form. As discussed above, the films deposited at 400°C are crystalline and the film surfaces become rough. So, the decrease in ionic conductivity at higher deposition temperatures is likely to be due to the crystallization of the films.

The inset of Fig. 4 shows the corresponding impedance plots as a function of deposition temperature. It is worthwhile to note that at higher temperatures, i.e. at 400 and 450°C, semicircles are more depressed. Considering the rough surface and crystallized structure, grain boundaries are likely to have formed, which will introduce additional resistance and capacitor effect.[14] Thus, it is likely that grain boundaries explain the more complex impedance characteristics of $Li_3PO_4$ films deposited at higher temperatures.

The electrochemical stability of $Li_3PO_4$ films grown at 300°C has been examined by CV in a Pt/$Li_3PO_4$/Li half-cell configuration. Fig. 5 shows the CV curve at a scan rate of 1 mV/s in the voltage range of −0.1 and 4.8 V. In the high potential range (from 2.0 to 4.8 V) no clear peaks can be observed. During the negative scan toward lower potentials, a large cathodic current is observed at −0.1 V (peak A) where lithium ions are reduced at the surface of the Pt layer to form Li–Pt alloys. As a result, two anodic peaks become visible in the reverse scan at 0.62 V (peak B) and 1.38 V (peak C). These peaks can be attributed to a two-step de-alloying process of Li–Pt,[8] where peaks B and C correspond to

$$2\,LiPt \rightarrow LiPt_2 + Li^+ + e^- \qquad [2]$$

$$LiPt_2 \rightarrow 2\,Pt + Li^+ + e^-, \qquad [3]$$

respectively. The inset of Fig. 5 shows the CV in the higher potential range from 1 to 5 V to avoid the Li-Pt alloy formation. The current never exceeds 1 μA/cm$^2$ in this potential range. However starting from 4.8 V, the anodic current increases rapidly, which is probably due to the oxidation of the solid electrolyte. It can therefore be concluded that the electrochemical stability of the deposited $Li_3PO_4$ films is in a range from 0 to 4.7 V vs Li/Li$^+$. Compared to nitrogen doped lithium phosphate (LiPON), the stability window of present MOCVD grown films is somewhat narrower but consistent with the previously reported values for $Li_3PO_4$ films deposited by laser deposition[8] and larger than for the reported RF-sputtered films.[4] The present electrochemical stability window is, however, large enough for most of the cathode materials used in all-solid-state batteries.

The volumetric storage capacity and rate capability are key properties for micro-batteries. Batteries with a three dimensional design would significantly improve the storage capacity due to the enlarged surface area.[1] In addition, compared to planar micro-batteries, the geometric current density of 3D batteries can be significantly lower because of the enlarged surface area, thereby dramatically improve the rate capability. The key issue of making structured micro-batteries is, however, the homogeneous deposition of the various battery components in 3D. To investigate this possibility for the present solid-state electrolyte, $Li_3PO_4$ has been deposited on 3D substrates and the uniformity of the deposited films has been investigated. The used 3D substrates consisted of silicon with etched trenches. Both the depth and width of the trenches are 30 μm as shown in Fig. 6a.

Although in the entire deposition temperature range, there is no significant difference in growth rate of $Li_3PO_4$, the lowest deposition temperature (300°C) was chosen, based on the good electrochemical performance of these films. As shown in Fig. 6b, the thickness of the $Li_3PO_4$ film at the top surface is continuous and homogeneous with a thickness of 340 nm. However, the film thickness quickly decreases to 210 nm just 1 μm away from the top-corner, which indicates that the deposition process is strongly diffusion-controlled. Comparing Fig. 6b and 6c, it becomes apparent that the film thickness decreases continuously with distance from the top surface increases. At the bottom (Fig. 6d) the $Li_3PO_4$ layer is no longer continuous.

Fig. 7 shows the film thickness development as a function of depth inside the trenches. At the top surface the film thickness appears to be

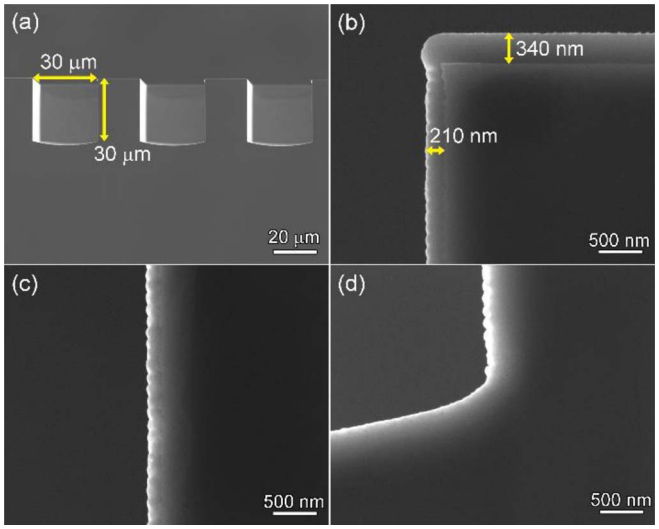


**Figure 6.** $Li_3PO_4$ thin film morphology deposited at 300°C for 6 h inside a 30 μm wide trench (a) and at higher magnification at the top (b), the center (c) and bottom (d).

quite constant. There is, however, a sharp and almost instantaneous thickness drop inside the Si trench followed by a more continuous decrease. At the bottom, the film thickness is about 75 nm, which amounts to 22% of the thickness at the top surface. As the deposition of $Li_3PO_4$ is a transport-controlled process, the growth of the film is limited by the diffusion of the mixed precursor gasses. Compared with the precursor gasses concentration at the top surface, the concentration inside the trenches decreases quickly and hence the layer thickness of the deposited $Li_3PO_4$ films will obviously become thinner. Based on the planar kinetic study (Fig. 1) and the 3D depositions, it can be concluded that using t-BuLi and TMPO as precursors under the present deposition conditions, MOCVD is not optimal to deposit $Li_3PO_4$ homogeneously for 3D micro-batteries.

Silicon is a promising anode material due to its high specific and volumetric energy density.[15] In addition, silicon is a competitive candidate to replace metallic lithium electrodes in micro-batteries, which suffer from a very low melting point. However, the large volumetric changes induced by the (de)lithiation process and the continuous loss and regeneration of the solid electrolyte interface (SEI) limits its practical application. Here, the MOCVD-deposited planar $Li_3PO_4$ films are introduced as a protective layer to isolate the Si anode from direct contact with the liquid electrolyte. As shown in Fig. 8a, the storage

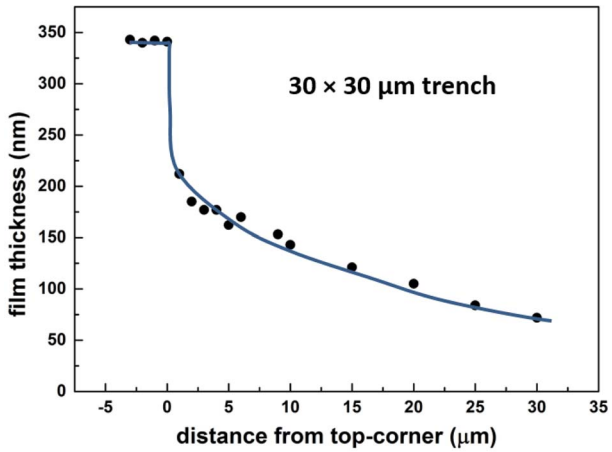


**Figure 7.** The development of the $Li_3PO_4$ film thickness as a function of distance from the top surface.

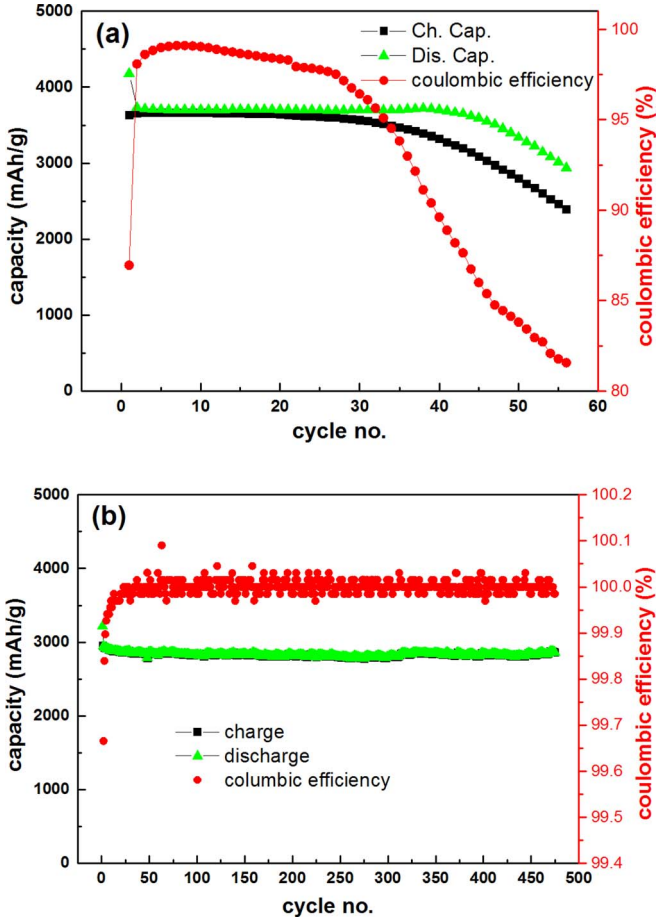


**Figure 8.** Cycle life performance of a 50 nm thickness Si film anode without (a) and with $Li_3PO_4$ (200 nm) protection (b).

capacity of the unprotected Si anode decays very quickly. After 55 cycles, about 35% of the initial capacity has been lost and the coulombic efficiency dropped to 81%. However, for the $Li_3PO_4$-protected Si anode hardly any capacity loss can be observed even up to almost 500 cycles. The coulombic efficiency of $Li_3PO_4$-protected Si is close to 100% and is very stable after the initial activation cycles. Such a high coulombic efficiency indicates that there are almost no side reactions occurring during charging and discharging.

The capacity-voltage curves of Si anodes without and with $Li_3PO_4$ protection are shown in Fig. 9a and 9b, respectively. The capacity of the Si electrode without $Li_3PO_4$ protection quickly shifted to lower values after 30 cycles. However, for the $Li_3PO_4$-protected Si electrode, after 400 cycles, the capacity-voltage curve still overlaps with previous ones, indicating that the $Li_3PO_4$-protected Si anode is indeed not attacked during the entire cycling performance test. Due to the well attachment between $Li_3PO_4$ and Si layers and good mechanical stability of the deposited lithium phosphate films, the $Li_3PO_4$-protected Si electrodes mainly expands perpendicular to the surface as reported previously.[16] As a result, the $Li_3PO_4$ film is homogeneously lifted rather than cracked and effectively protects the Si anode film from the attack of liquid electrolyte.

It is worthwhile to note that both first cycles (black curves) are somewhat different from the other cycles. For unprotected Si electrode, this deviation comes from SEI formation. For the $Li_3PO_4$-protected Si electrode, an additional reduction peak only appears in the first cycle (indicated by the arrow), which may be attributed to the activation of the Si/$Li_3PO_4$ interface as has been reported before.[17] Obviously, a MOCVD-deposited thin film of $Li_3PO_4$ with a thickness of only 200 nm fully suppresses the SEI formation and

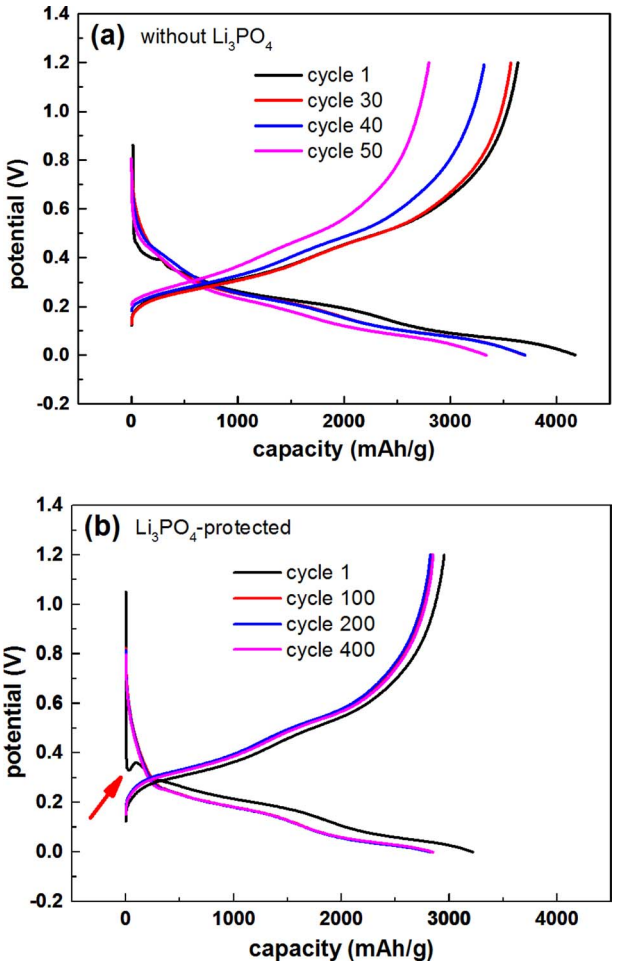


**Figure 9.** Capacity-voltage curves of Si anodes without (a) and with $Li_3PO_4$ protection (b).

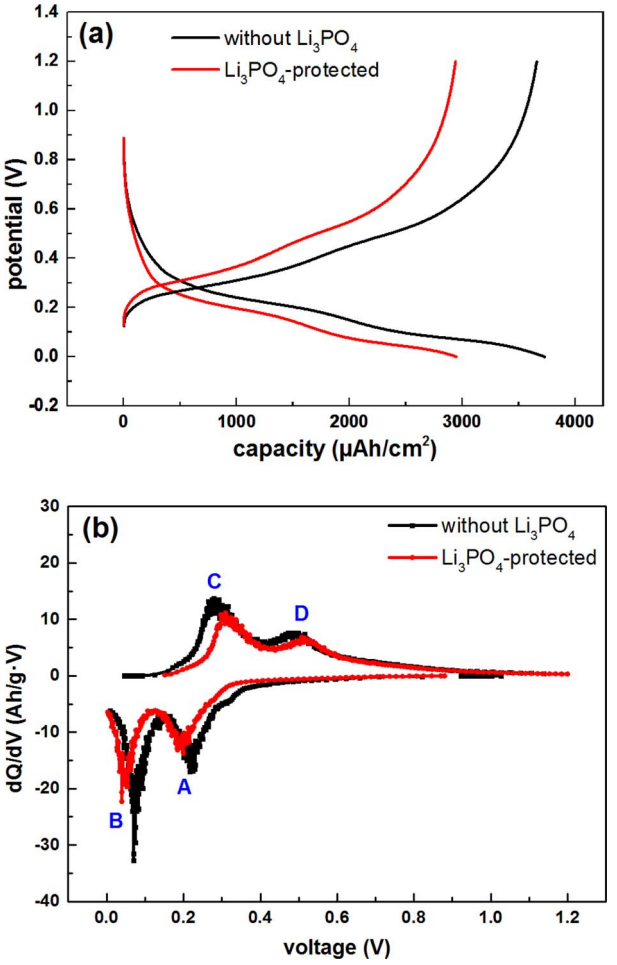


**Figure 10.** Capacity-voltage curves (a) and derivative of storage capacity with respect to voltage curves (b) for unprotected and protected Si electrodes at cycle 2.

dramatically improves the cycle life performance of Si thin film electrodes.

Furthermore, it is interesting to note that after covering the Si electrode with a $Li_3PO_4$ film, the initial storage capacity of the Si anode is somewhat lower than that of the uncovered electrode. This may be due to the additional resistance introduced by the solid-state electrolyte. In order to investigate this influence, the capacity-voltage curves of the second (dis)charging cycle have been investigated. To avoid the influence of the SEI formation in the case of the unprotected electrode and the activation process in the case of $Li_3PO_4$-protected electrode, the second cycle has been compared. Fig. 10a shows that the overpotentials for the $Li_3PO_4$-protected Si electrode during (dis)charging are higher than for the unprotected electrode. This is also confirmed by the derivative of storage capacity with respect to the voltage curves shown in Fig. 10b. Two reduction peaks (A and B) are observed, which correspond to the transition of Si into amorphous lithium silicides.[18] Correspondingly, two oxidation peaks (C and D) are found during the oxidation process. Compared to the unprotected electrode, the reduction peaks of the $Li_3PO_4$-protected Si electrode shifted to lower potentials and the oxidation peaks to higher potentials.

Conclusively, Fig 10b clearly indicates that the $Li_3PO_4$-protected electrode reveals similar (de)lithiation processes, which are characteristic for Si anodes. But due to the additional resistance introduced by the $Li_3PO_4$ film, the overpotentials are somewhat increased, resulting in the observed virtual capacity loss. However, given the improved cycle-life performance, such a capacity sacrifice is very acceptable, because after 50 cycles the $Li_3PO_4$-protected electrode actually already has a much higher storage capacity. The $Li_3PO_4$ film thickness on the Si electrode for which the results are given in Fig. 8b is only 200 nm, which apparently is pinhole-free and sufficient to protect the underlying Si electrode. The extraordinary performance of $Li_3PO_4$-protected Si thin film electrode also shows the excellent mechanical and electrochemical stability of the MOCVD-deposited $Li_3PO_4$ film.

## Conclusions

Lithium phosphate thin-film solid-state electrolytes were successfully deposited by MOCVD. The $Li_3PO_4$ film deposited at 300°C shows the highest ionic conductivity of $3.9 \times 10^{-8}$ S · cm$^{-1}$. As the deposition temperature increases, the surface morphology of the deposited films becomes more rough. XRD results show that $Li_3PO_4$ starts to crystallize when the deposition temperature increases beyond 350°C. The ionic conductivity of these films quickly decreases to lower values when the deposition temperature increases. A kinetic study on planar substrates indicates that the growth of $Li_3PO_4$ films is a diffusion-controlled process. This is confirmed by investigating the thickness development of the deposited thin films inside 3D-structures. MOCVD-deposited $Li_3PO_4$ films are shown to be a very effective protective layer for Si electrodes. Solid-state electrolytes with a thickness of only 200 nm can completely suppress the SEI formation and improve the cycle life performance of Si electrodes strikingly.

## Acknowledgments

This work was supported by IWT Flanders (Belgium) under SBO project "SoS-Lion".

## References

1. P. H. L. Notten, F. Roozeboom, R. A. H. Niessen, and L. Baggetto, *Adv Mater*, **19**, 4564 (2007).
2. J. F. M. Oudenhoven, R. J. M. Vullers, and R. Schaijk, *Int. J. Energy Res.*, **36**, 1139 (2012).
3. D. Golodnitsky, M. Nathan, V. Yufit, E. Strauss, K. Freedman, L. Burstein, A. Gladkich, and E. Peled, *Solid State Ion.*, **177**, 2811 (2006).
4. X. H. Yu, J. B. Bates, G. E. Jellison, and F. X. Hart, *J Electrochem Soc*, **144**, 524 (1997).
5. J. B. Bates, N. J. Dudney, G. R. Gruzalski, R. A. Zuhr, A. Choudhury, C. F. Luck, and J. D. Robertson, *J Power Sources*, **43**, 103 (1993).
6. J. B. Bates, N. J. Dudney, G. R. Gruzalski, R. A. Zuhr, A. Choudhury, C. F. Luck, and J. D. Robertson, *Solid State Ion.*, **53**, 647 (1992).
7. H. Y. Park, S. C. Nam, Y. C. Lim, K. G. Choi, K. C. Lee, G. B. Park, S. R. Lee, H. P. Kim, and S. B. Cho, *J. Electroceram.*, **17**, 1023 (2006).
8. N. Kuwata, N. Iwagami, Y. Tanji, Y. Matsuda, and J. Kawamura, *J Electrochem Soc*, **157**, A521 (2010).
9. W. Y. Liu, Z. W. Fu, C. L. Li, and Q. Z. Qin, *Electrochem. Solid State Lett.*, **7**, J36 (2004).
10. L. Meda and E. E. Maxie, *Thin Solid Films*, **520**, 1799 (2012).
11. J. Hamalainen, J. Holopainen, F. Munnik, T. Hatanpaa, M. Heikkila, M. Ritala, and M. Leskela, *J Electrochem Soc*, **159**, A259 (2012).
12. H. T. Kim, T. Mun, C. Park, S. W. Jin, and H. Y. Park, *J Power Sources*, **244**, 641 (2013).
13. J. F. M. Oudenhoven, T. van Dongen, R. A. H. Niessen, M. H. J. M. de Croon, and P. H. L. Notten, *J Electrochem Soc*, **156**, D169 (2009).
14. J. T. S. Irvine, D. C. Sinclair, and A. R. West, *Adv Mater*, **2**, 132 (1990).
15. P. H. L. Notten, F. Roozeboom, R. A. H. Niessen, and L. Baggetto, *Adv Mater*, **19** (2007).
16. P. Viet Phong, P. Brigitte, and C. Frédéric Le, *Adv Funct Mater*, **22** (2012).
17. L. Baggetto, R. A. H. Niessen, and P. H. L. Notten, *Electrochim. Acta*, **54**, 5937 (2009).
18. J. P. Maranchi, A. F. Hepp, and P. N. Kumta, *Electrochemical and Solid-State Letters*, **6** (2003).